JOURNAL OF MATERIALS SCIENCE 23 (1988) 3732–3743

Fatigue behaviour of hybrid composites:

Part 1 *Carbon/Kevlar hybrids*

G. FERNANDO, R. F. DICKSON*, T. ADAM, H. REITER, B. HARRIS
Schools of Materials Science and Mechanical Engineering, University of Bath, Bath BA2 7AY, UK

A study has been made of the fatigue behaviour of carbon/Kevlar-49/epoxy hybrid composites. Stress–life data have been obtained for both unidirectional and $[(\pm 45, 0, 0)_2]_s$ laminates in repeated tension and compression–tension cycling tests at various values of the stress (or R) ratio. Goodman (constant life) diagrams are presented for the unidirectional composites which indicate that the fatigue resistance of hybrid mixtures varies linearly with composition. The presence of the Aramid fibre, whose natural resistance to compression loads is suspect, does not appear to exert any unexpected damaging influence on the response of the hybrids either in tensile or tension–compression loading. This is also true of the behaviour of hybrid laminates containing plies at an angle to the main loading direction.

1. Introduction

The concept of hybrid, or mixed fibre, composites is a natural extension of the composites principle of combining materials to optimize their value to the engineer. Mixing two or more types of fibre in one matrix allows even closer tailoring of composite properties to suit specific requirements than can be achieved with a single fibre species. Some hybrids of current interest represent attempts to reduce the cost of composites with expensive reinforcements by incorporating a proportion of cheaper, lower-quality fibres without too seriously reducing the mechanical properties of the original composite. However, of equal importance is the reverse principle, that of improving the stiffness of, say, a glass reinforced plastic (GRP) structure with a small quantity of judiciously placed carbon or Kevlar-49 aromatic polyamide fibre, without inflicting too great a cost penalty. In high-technology fields the question of cost may be insignificant by comparison with the advantages of optimizing properties. In aerospace applications, for example, one of the most important purposes of using hybrids is to utilize the natural toughness of Kevlar (Aramid) or glass fibre reinforced plastics to offset the relative brittleness of typical carbon fibre composites (CFRP). An often-debated issue is whether or not it is possible to obtain greater improvements in some properties than might be predicted from calculations based upon properties of the separate components.

2. Fatigue resistance of hybrids

In attempting to predict the $S/\log N$ behaviour of, say, a carbon–glass hybrid, the obvious starting point would be the $S/\log N$ fatigue curves for plain CFRP and GRP of comparable structure. For most CFRP the curve will be relatively flat, with a slope which, for a given fibre volume fraction, V_f, is greater the lower the modulus of the reinforcing fibre. This is in accordance with the supposition that the stiffer the fibre, the less likely it is that strain levels sufficiently high to damage the resin or interface will be developed during cycling, even at high stresses. By the same argument, the $S/\log N$ curve for GRP falls more steeply and with greater curvature. The $S/\log N$ curves for glass–carbon hybrids will then be interpolated between these two extremes, as Phillips [1] and Hofer *et al.* [2] have shown, and the higher the carbon content, the greater the fatigue resistance. Phillips' results show that for carbon–glass cloth hybrids the increase in tensile fatigue strength (for a life of 10^5 cycles, for example) is proportional to the glass–carbon ratio. This pattern of behaviour would be expected to be sensitive to the scale of the hybridization or the intimacy of mixing of fibres which should determine the extent to which the mode of failure of the weaker component is modified or even suppressed by the presence of the stronger. It has been suggested, for example, that interply hybridization is likely to be superior to core–shell combinations [3]. However, it does not necessarily follow, at the other extreme, that intimate mixtures of the kind described by Parratt and Potter [4] would in turn be superior to interply hybrids.

Of special interest is the likely effect of Aramid fibre on the performance of a hybrid containing it in combination with some other composite of known high fatigue resistance, such as CFRP. We have previously reported on an undesirable kind of behaviour of 0/90 Kevlar/epoxy (KFRP) composites under repeated tension loading [5]. Fig. 1 shows that the fatigue curve for such a laminate (presented as initial strain plotted against life) has a steeply descending characteristic with a drastic shortening of the fatigue life for strains

* *Current address*: Alcan International Banbury Laboratories, Oxon, UK.

 0022–2461/88 $03.00 + .12

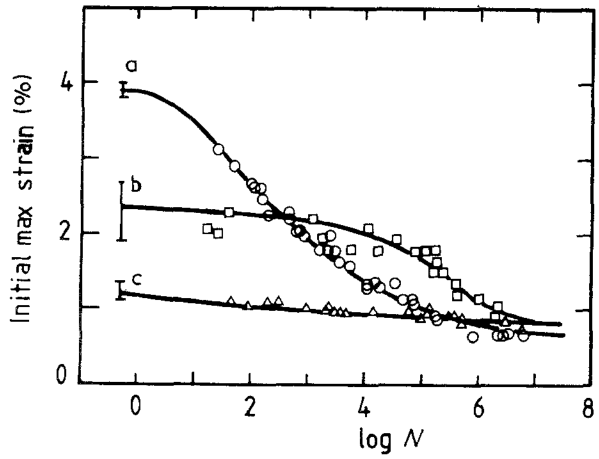

Figure 1 Strain against log life curves for 0/90 laminates of (a) GRP (b) KFRP and (c) CFRP (after Jones *et al.* [5]).

corresponding to stress levels below about 90% of the tensile failure stress. The behaviour of the three comparable materials for which results are given in Fig. 1 (i.e. CFRP, GRP and KFRP, all of 0/90 construction and containing the same epoxy resin) falls, nonetheless, into a pattern which can be interpreted in terms of a model developed by Talreja [6].

The low slope of the strain–life curve for the CFRP implies that the working strains in the composite are only marginally above the natural endurance limit of the matrix resin, the high cyclic stresses being sustained by fibres in the 0° plies. The same failure mechanism operates over the whole range of fatigue strains, with gradual deterioration of the load-bearing ability of the 0° plies through statistically determined fibre breakage. In the case of the GRP, the high strain level engendered by the compliant fibres promotes early failure by mixed-mode damage mechanisms, matrix cracking and interfacial shear, at almost all strain levels. This results in the characteristic steep slope of the strain–life (and of the $S/\log N$) curve which ultimately falls to approximately the same level as the CFRP curve for lives beyond about 10^6 cycles at the intrinsic matrix fatigue limit.

The KFRP strain–life curve shows behaviour intermediate between these two extremes. The fibre compliance is greater than that of the XAS carbon, but the fatigue behaviour of the composites, for lives less than about 10^5 cycles, is as good as that of the CFRP, the slope of the strain–life curve being approximately the same. In this flat initial region composite failure is determined, following Talreja, by breakage of the 0° fibres accompanied by interfacial debonding. Beyond this number of reversals, however, the curve takes a downward turn. In Talreja's model, this implies a change of controlling mechanism from fibre breakage to matrix cracking accompanied by interfacial shear, and the curve is expected to continue falling until it reaches the intrinsic matrix fatigue limit when it should level out and become coincident with the GRP and CFRP curves for lives greater than about 10^7 cycles.

Although there is apparently a change in mechanism involved in determining the shape of the KFRP curve, Talreja's interpretation does not seem appropriate. We prefer to interpret the downward trend in terms of an additional mechanism of degradation of fibre strength through local surface abrasion or internal disruption of the fibres as a result of the repeated loading–unloading sequence, and we are led to consider two possible consequences of this KFRP behaviour. The first is the possibility that any loading régime with a significant compression component could lead to even worse fatigue performance of the KFRP. The second is that in a carbon–Kevlar hybrid laminate, the apparent weakness of the Aramid component could detract from the otherwise excellent performance of the carbon component to a greater extent than would be predicted by, say, an elementary failure strain analysis [7], giving rise to what has sometimes been called a "negative hybrid effect". The work reported here is, therefore, concerned with the fatigue response of carbon–Kevlar–epoxy hybrids in tension–compression cycling over a wide range of values of the stress ratio, $R(\sigma_{min}/\sigma_{max})$.

3. Materials

Materials were supplied by Ciba-Geigy as zero-bleed prepregs of XAS carbon fibre and Kevlar-49 fibre in the same BSL 914 epoxy resin. Prepregs were laid up on a vacuum-assisted laying-up table according to pre-determined compositions and stacking sequences, and were autoclaved at the Royal Aircraft Establishment, Farnborough, following the manufacturer's recommendations. The laminate fibre volume fractions were nominally 60%.

3.1. Compositions and lay-ups

Two main lay-up geometries have been studied, the first being unidirectional, to provide a base-line of fibre-dominated performance for the various hybrids, and the second being $[(\pm 45, 0_2)_2]_s$ laminates. A smaller number of simple $[(\pm 45)_4]_s$ laminates were also prepared for comparison purposes.

The compositions of the unidirectional laminates were plain carbon, 25%, 37.5% and 50% by volume of Kevlar in carbon, and plain Kevlar. The hybrid lay-ups corresponding to these compositions were

(i) $(K, C, C, C, C, K, C, C)_s$
(ii) $(K. C, C, K, C, C, K, C)_s$
(iii) $[(K, C)_4]_s$

the deliberate intention being to maintain the outer plies of KFRP in all hybrid compositions. The lay-ups of the single-fibre laminates were 16-ply stacks, to match the overall structure of the hybrids.

The structural laminate chosen for the investigation was of the type $[(\pm 45, 0, 0)_2]_s$. Sixteen-ply plain carbon and plain Kevlar fibre composites were made up in this structure for comparison with the behaviour of a 50/50 carbon–Kevlar hybrid. The hybrid stacking sequence, which was determined by the composition rather than by normal structural considerations, was

$$[(\pm 45)K, 0C, 0K, (\pm 45)C, 0K, 0C]_s$$

The plies were mixed so as to arrange for all interfaces (except the $+45/-45$ interfaces) to be carbon–Kevlar interfaces.

The standard, autoclaved, 1.0 m × 0.3 m plates were

C-scanned after manufacture, following which they were dried and bagged to await use. The cutting of test samples was carried out in such a manner as to avoid the use of plate edges as well as areas indicated as defective by the ultrasonic scanning. Plain carbon laminates were cut to size for testing on a water-cooled diamond saw, while Kevlar-containing materials were cut by water-jet at British Hovercraft.

3.2. Environmental conditioning

We have previously studied the effects of environmental conditioning on the fatigue response of the three types of composite mentioned earlier [5]. It was found that, except under grossly exaggerated pretreatment conditions, the fatigue characteristics of the composites were not sensitive to the effects of hygrothermal treatment. For the current work, therefore, a standard conditioning routine was used to bring all materials to a moisture content of approximately 1% by room-temperature treatment in a 65% RH enclosure.

Differential thermal contraction, following cooling from the cure temperature, leads to residual thermal strains in hybrid laminates. However, a simple composite beam theory analysis, based on the known elastic and thermal properties of CFRP and KFRP, leads to the result that in a 50/50 carbon–Kevlar unidirectional hybrid the maximum possible level of compressive thermal stress in the KFRP plies would be of the order of only 20 MPa. This ply stress level would result in a Kevlar *fibre* stress of about 35 MPa in a 60 vol % ply which is of the order of 13% of the room-temperature compression yield stress of the Kevlar plies [8]. This level of residual stress would probably be eliminated during the environmental conditioning process, and would not, therefore, be expected to influence the fatigue properties of the hybrid. However, we note that another consequence of differential thermal contraction is that during the early stages of cooling, when the resin retains some capacity for plastic flow, the plies containing the fibres with the lower expansion coefficient (i.e. the Kevlar in a C–K hybrid) will buckle and remain so in the cured laminate.

4. Fatigue testing

For all tests involving a compressive stress component, a stabilization jig was used to prevent premature buckling failures in fatigue. With careful attention to setting up, in particular to the need for careful control of the packing between sample and jig, it was possible to obtain fatigue failures in the gauge length up to high levels of imposed compressive stress, although the jig was not suitable for the measurement of monotonic compression strengths and gave rise to difficulties at high cyclic frequencies. Static compression strengths of materials were measured, when needed, in Dr Andrew Barker's laboratory in the Chemical Engineering Department at Birmingham University.

Fatigue tests were carried out in a pair of Instron 1332 sevo-hydraulic machines operating under load control. In our previous work [5] we emphasized the need to ensure comparability of results for different composites by allowing for the strain-rate sensitivity of the strength of our three different types of material. With carbon and Kevlar reinforced plastics, however, the problem is less serious since, as we showed earlier, the tensile strengths of both CFRP and KFRP were found to be independent of testing rate. We have not, therefore, been constrained to run all tests at the same rate of load application, as in our last programme, and although the majority of the tests were carried out at a rate of load application of approximately 200 kN sec^{-1}, we increased the rate to 500 kN sec^{-1} where necessary to achieve a reasonable testing rate. A limited number of tests on the unidirectional carbon–Kevlar composites over this range of frequencies showed that there were no effects of frequency on fatigue response. It is also known that KFRP develop higher temperatures during fatigue testing as a result of hysteretic heating: we have, therefore, carried out a brief survey of the effect of testing at elevated temperature. Monitoring of the temperature rise during repeated tension cycling of unidirectional KFRP at ambient temperature showed that the maximum surface temperature occurring during any test was 40° C. The expected temperature rise in any hybrid would therefore be lower than this. In a series of tests on unidirectional KFRP laminates at 100° C, it was found that the S/log N curve obtained was indistinguishable from that obtained at 23° C.

All fatigue tests have been carried out on straight-sided (unwaisted) coupons, with their edges polished to remove the most serious cutting marks, and with soft aluminium end-tabs bonded on to prevent grip damage. These end-tabs were glued to the specimen surfaces, following shot-blasting of the aluminium and abrasion of the sample surface, with Redux 403 resin cured for 10 h at 45° C under light load.

5. Fatigue behaviour of unidirectional carbon–Kevlar hybrids

5.1. Mechanical properties

The tensile mechanical properties of this family of hybrids are shown as a function of nominal composition in Fig. 2, from which it can be seen that the stiffness varies linearly with Kevlar content, and the tensile strength varies in the manner expected from the constant strain model [7]. The similarity of the failure strains of the CFRP and KFRP means that there is no possibility of what is normally termed a "hybrid effect", i.e. of an apparent enhanced failure strain in the CFRP component [9].

5.2. Fatigue behaviour

Cyclic testing of the conditioned samples was carried out over a range of R values from $+0.5$ to -1.2, although not all R values were covered for all hybrid compositions. Fig. 3 shows results for plain CFRP samples plotted as peak (tensile) stress plotted against log life: it illustrates an *apparent* reduction in life of the composite in the presence of a compressive stress component. The slope of the S/log N curve for $R = 0.1$ is approximately 82 MPa $decade^{-1}$, or 4.2% of the monotonic fracture stress per decade.

As Fig. 4 shows, the $R = 0.1$ curve for plain KFRP is also qualitatively similar in shape to that obtained

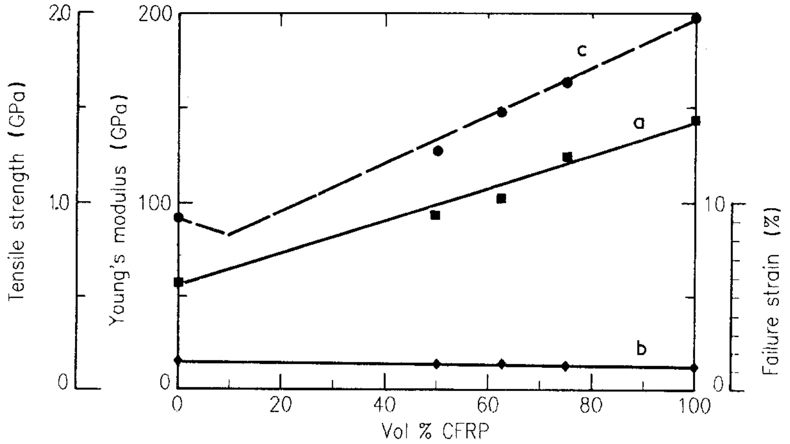

Figure 2 Mechanical properties as functions of composition in the unidirectional XAS carbon–Kevlar hybrid system. The dashed line represents the predictions of strength given by the simple constant strain model [7] (a Young's modulus, b failure strain, c tensile strength).

for the 0/90 KFRP in our earlier study [5] (Fig. 1) although the deterioration resulting from the failure mode change originates earlier and appears to be less drastic in the 0/90 laminate. The difference is likely to be due to the presence of the transverse plies and their effect in generating damage in the 0° fibres earlier in the life of the 0/90 composite. In both cases there is a slight worsening of fatigue resistance when the R ratio is changed from +0.1 to +0.01 although both regimes are, macroscopically at least, repeated tension modes of cycling. The effects of introducing a compressive component of cycling are also seen from Fig. 4 to be more drastic for the KFRP than for CFRP, although the comparison is only qualitative in these peak stress against life plots which give no direct indication of the true range of strain to which the sample is being subjected when R is less than zero.

Fig. 5 shows data for the 37.5% KFRP–CFRP hybrid, again in terms of peak stress plotted against life. The curves for the different R ratios are clearly separated, but they cannot be extended back to the ordinate to link with the monotonic strength values because those data have no relevance in a peak-tensile-stress $S/\log N$ plot. Fig. 6 illustrates the effect of hybrid composition on the shape and disposition of the $S/\log N$ curve for repeated tension cycling (R = 0.1). There appears to be a uniform variation between the two extremes, the almost linear $S/\log N$ curve for CFRP gradual giving way to the marked two-stage behaviour characteristic of the KFRP as the Aramid fibre content increases.

To demonstrate the effect of the compressive stress component on the hybrid strain–life curves, the results may be plotted in terms of alternating strain *range*, $\Delta\varepsilon_{alt}$, as shown for the three hybrid compositions in Fig. 7. The data are scattered and there is no easily discernable trend other than a slight increase in slope as the Aramid content increases. For lives beyond about 10^5 cycles the working strain range is almost constant, regardless of composition. The average value of $\Delta\varepsilon_{alt}$ for a life of 10^5 cycles, for example, for all three hybrid compositions and the two single fibre composites, and for all R values, is 1.08% with a coefficient of variation of only 14% (16 separate sets of data). Even at this stage of the evaluation, therefore, there do not appear to be any unusual effects either of the presence of the Aramid fibre in the hybrids or of the high compression stress component of cycling.

The $S/\log N$ curves for the unidirectional hybrids were used to prepare the constant life (Goodman) diagram, shown in Fig. 8, which relates to a life of 10^5 cycles. The diagram shows a number of important features. The first is the asymmetry of the diagram, a familiar feature of such diagrams for composite materials [10] which indicates the loss of fatigue resistance under cycling régimes that include a compressive stress component, a consequence of the reduced load-bearing ability of composites under static compressive loads. The second feature is the similarity of the forms of the curves for the four composites represented in the diagram, which again indicates that the Aramid fibre is exerting no unexpected weakening effect on the fatigue response of the CFRP in the hybrid laminate.

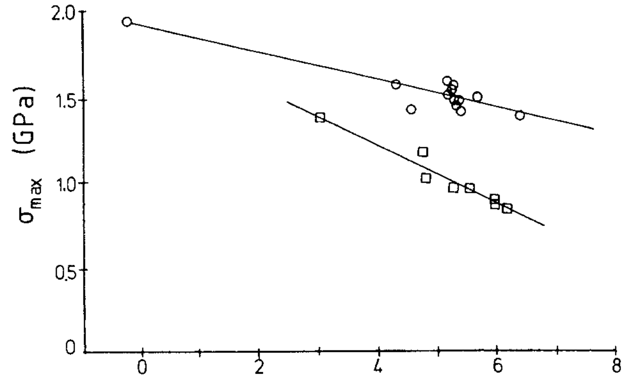

Figure 3 Effect of R ratio on the $S/\log N$ curves of unidirectional CFRP laminate (XAS/914). The stress levels plotted are the peak stresses in the cycle. (○) R = 0.1, (□) R = −0.6.

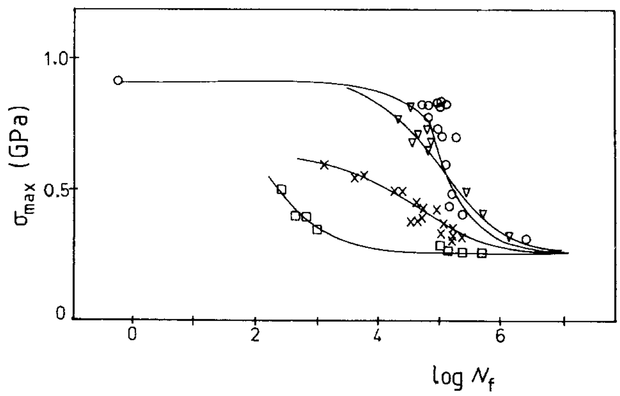

Figure 4 Effect of R ratio on the $S/\log N$ curves of unidirectional KFRP laminate (Kevlar/914). (○) R = 0.1, (▽) R = 0.01, (x) R = −0.3, (□) R = −0.6.

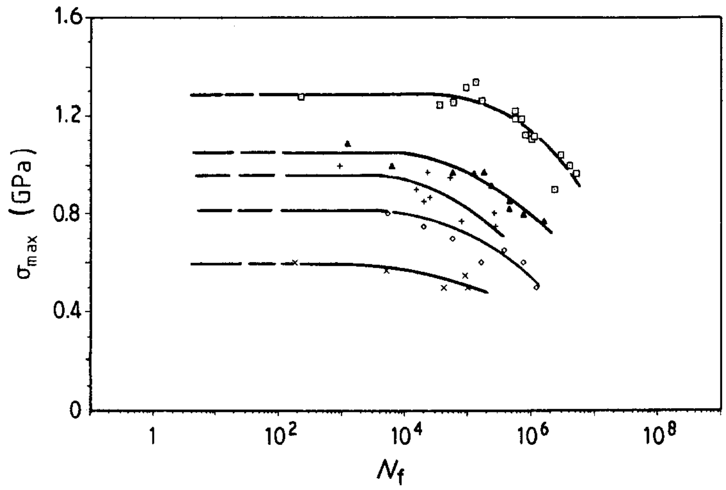

Figure 5 Effect of R ratio on the S/log N curves of unidirectional carbon–Kevlar hybrid (38% Kevlar). (□) R = 0.1, (▲) R = −0.3, (+) R = −0.6, (◇) R = −0.8, (x) R = −1.2.

The data from the S/log N curves are cross-plotted to illustrate the variation of fatigue response with composition in Figs 9a and b which show the peak stress plotted against composition for lives of 10^5 and 10^6 cycles, respectively. Within the level of scatter of the original results, the fatigue response, like the tensile properties, varies linearly with composition as in the case of the woven glass–carbon hybrids discussed by Phillips [1]. This holds true both for all-tension cycling and where there is a significant compressive stress component. The whole family of composites is weaker in compression than in tension, but this weakness is no greater for the plain KFRP or for hybrids containing a substantial proportion of Aramid than it is for plain CFRP.

The fact that the curves of Fig. 10, showing fatigue stress (for a given life) as a function of hybrid composition, are roughly linear suggests, as we have said, a uniform variation of fatigue resistance as the composition changes from plain KFRP to plain CFRP. Implicit in such an interpretation, however, is the idea that the base-line for such comparisons is the notional rule of mixtures. We have shown earlier that the strengths of these unidirectional hybrids fall close to the predictions of the iso-strain model of hybrid behaviour (Fig. 2) which are slightly below mixtures rule values. A better means of comparing the fatigue resistance of the hybrids is by the use of the familiar fatigue ratio, the fatigue stress for a given life divided by the monotonic tensile strength, which effectively normalizes the results of Fig. 9. This can logically only be done for the R = 0.1 results, and Fig. 10 shows the effect of this normalizing procedure on the data for lives of 10^5 and 10^6 cycles. A completely different picture now emerges, since the two curves in this figure are no longer linear interpolations between the two end points. For none of the hybrid compositions investigated (i.e. up to 50 vol % KFRP in CFRP) does

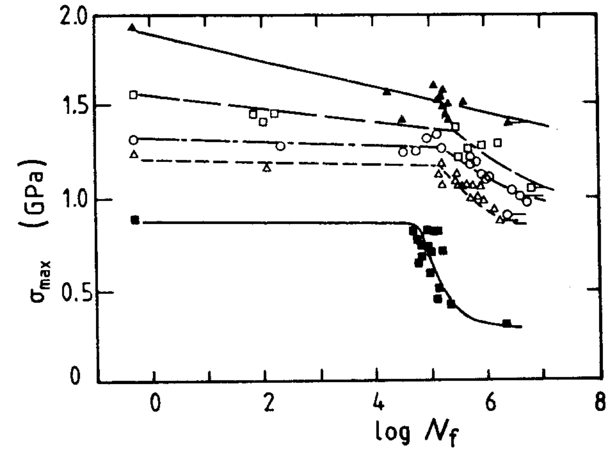

Figure 6. S/log N curves (peak stresses) for the whole family of unidirectional carbon–Kevlar hybrids, including the plain XAS and plain Kevlar materials. The curves are drawn by eye for best fit. (R = 0.1) (▲) CFRP; (□) 25% K; (○) 35% K; (△) 50% K; (■ KFRP)

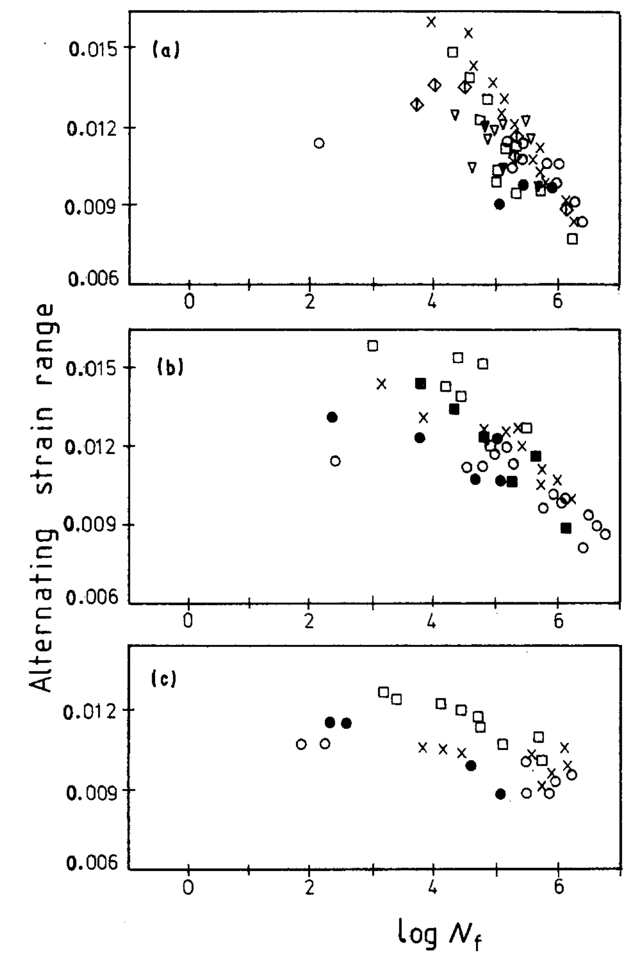

Figure 7 Fatigue results for the unidirectional carbon–Kevlar hybrids plotted in terms of the total (alternating) strain range against log life, showing the effect of the R ratio (a) 50% KFRP (b) 38% KFRP (c) 25% KFRP. (○) R = 0.1, (▽) R = 0.01, (◇) R = −0.1, (x) R = −0.3, (▼) R = −0.4, (□) R = −0.6, (■) R = −0.8, (●) R = −1.2.

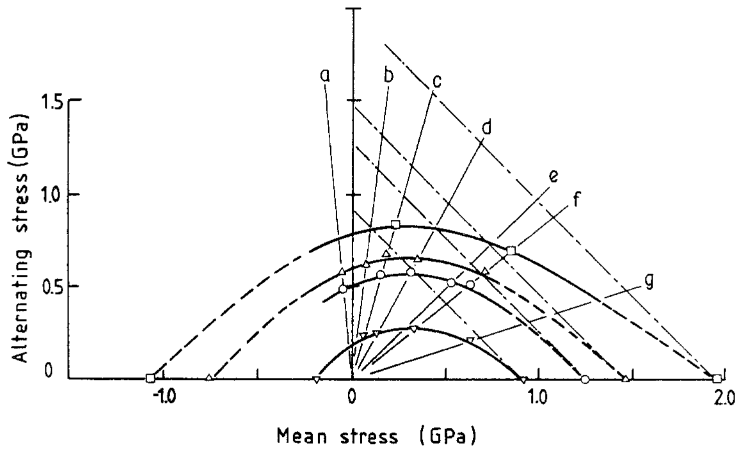

Figure 8 Constant life (Goodman) diagram for the effect of mean stress on the fatigue response of unidirectional carbon–Kevlar hybrids. The alternating stresses plotted represent the peak stress values for failure in 10^5 cycles. The broken lines at 45° represent the limits for tensile failure. (□ all carbon, △ 38% Kevlar, ○ 50% Kevlar, ▽ all Kevlar). (a) $R = 1.2$, (b) $R = -0.8$, (c) $R = -0.6$, (d) $R = -0.3$, (e) $R = 0.01$, (f) $R = 0.1$, (g) $R = 0.5$.

the addition of Aramid fibre result in a reduction in the composite fatigue ratio. For lives of 10^6 cycles, despite the fact that the plain KFRP perform badly at this level, the fatigue ratio is unchanged by the KFRP additions. For the shorter life (10^5 cycles) the ratio even increases with Kevlar content. From these results, however, we cannot comment on the likely effect of adding more than 50 vol % of KFRP.

5.3. Fractography

Post-failure surface examination is an unsatisfactory method of obtaining information on fatigue damage mechanisms in composites since the broken samples usually sustain additional damage after failure. However, provided the samples are carefully prepared, useful information may still be obtained from surface damage analysis. Our fractography studies suggest that the observed failure modes can give an indication of the loading history of the specimen. There is also evidence in favour of the Talreja damage model [6].

The most prominent macroscopic features of samples of unidirectional carbon and Kevlar composites tested to failure in monotonic tension are longitudinal splitting and transverse failure near end-tab regions. When the same materials are tested in repeated tension fatigue the extent of this splitting is dependent on the peak stress level in the cycle. Samples fatigued at stresses of the order of 80–90% of the static failure load resembled those tested monotonically to failure, while at lower stress levels larger numbers of splits were observed. The failure mode is modified when there is a compressive stress component in the fatigue cycle, with less longitudinal splitting and the occurrence of extensive delamination, perhaps encouraged by the pre-buckled state of the fibres. Outer Kevlar plies delaminate and then fracture into short, discrete lengths. Although, as we have said, there was no change in the fatigue response when samples were tested at 100° C, there were differences in the failure mode, the outer Kevlar plies failing in a manner more typical of monotonic tensile failure, with longitudinal splitting, and with the final failure of the Kevlar plies, following delamination, being localized in the centre region of the sample.

Fracture surface features of samples fatigue tested

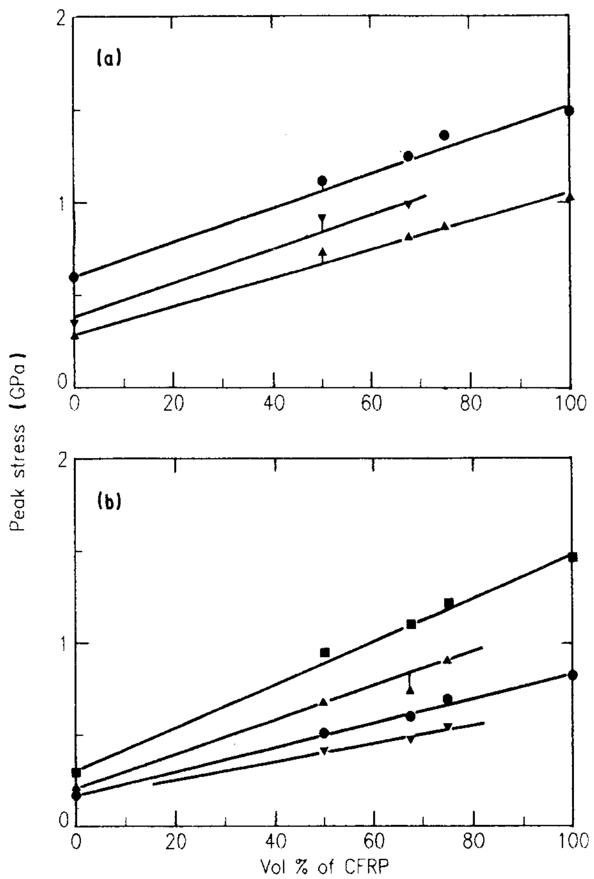

Figure 9 Effect of composition on the fatigue response of unidirectional carbon–Kevlar hybrids, showing the effect of R ratio. (a) is for a life of 10^5 cycles (●) $R = -0.1$, (▼) $R = -0.3$, (▲) $R = -0.6$), (b) for 10^6 cycles (■) $R = 0.1$, (▲) $R = -0.3$, (●) $R = -0.6$, (▼) $R = -1.2$).

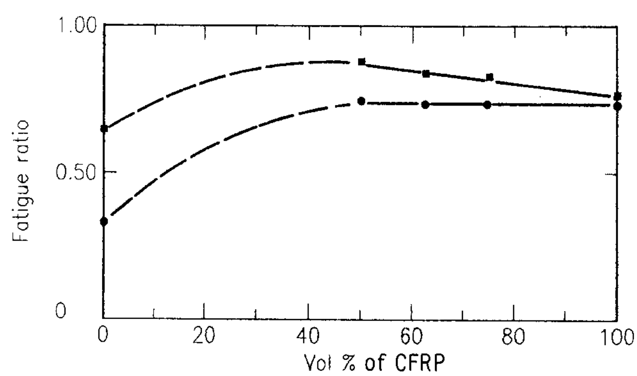

Figure 10 Fatigue ratio as a function of hybrid composition for unidirectional carbon–Kevlar hybrids. The fatigue ratio is the fatigue stress for a given life (data for 10^5 (■) and 10^6 (●) cycles from Fig. 9) divided by the monotonic tensile strength (from Fig. 1) ($R = 0.1$).

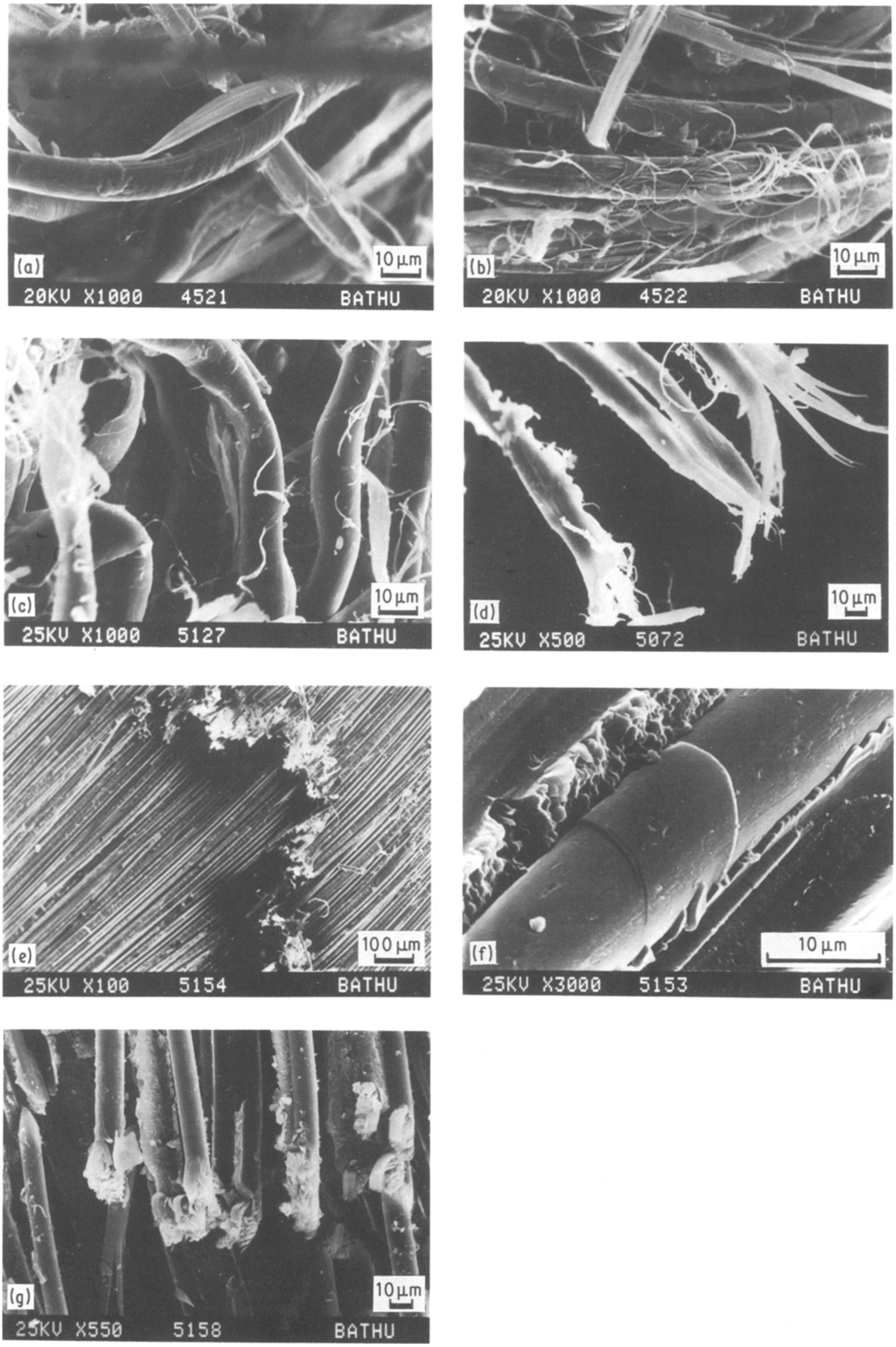

Figure 11 Scanning electron micrographs of fracture surfaces of fatigued unidirectional KFRP samples. For descriptions, see text.

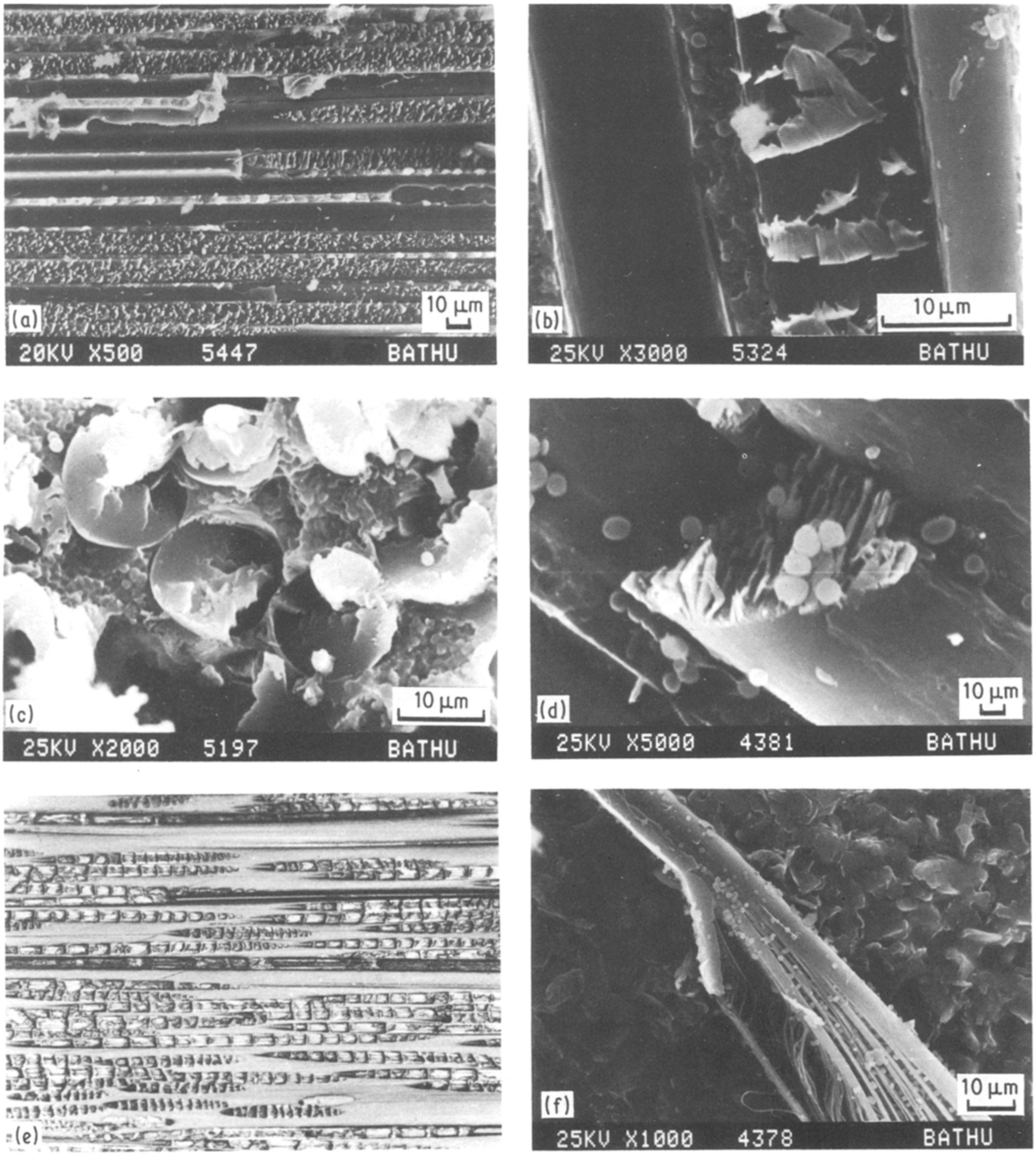

Figure 12 SEM photographs of fracture surfaces of fatigued CFRP/KFRP hybrids, together with one optical micrograph (12e). For descriptions, see text.

in repeated tension are similar to those commonly observed, the surfaces of the carbon plies being relatively plane, with no signs of pull-out, and the Kevlar plies showing extensive defibrillation. When the outer Kevlar plies were able to bend as a result of delamination the individual fibres sustained characteristic bending and fretting damage as indicated by the multiple kinking and shredding visible in Figs 11a and b. With increasing magnitude of compressive component during cycling, extensive local buckling of the Kevlar fibres becomes apparent and final failure is often by fibre core–skin separation (and pull-out) as illustrated in Figs 11c and d. The longitudinal surfaces of outer plies in samples tested in tension-compression showed characteristic evidence of kink-initiated failure (Fig. 11e) associated with visible microstructural damage in the individual fibres (Fig. 11f). Brush-like damage to the ends of fibres, typical of that expected from impacted fibre ends following a planar fracture, can be seen in Fig. 11g.

When the Kevlar plies are sandwiched between carbon plies instead of being outer plies, the damage mechanisms are again different. Figs 12a and b illustrate damage that we consider to be due to abrasion. Under the influence of very high compressive stress components the failure mode of the Kevlar plies is totally changed, exhibiting the planar failure surface features normally associated with the more brittle CFRP component, as shown in Fig. 12c. Sometimes the individual fibres show completely flat, pseudo-brittle failure

TABLE I Mechanical properties of $[(\pm 45, 0_2)_2]_s$ carbon, Kevlar and hybrid laminates

Laminate	Tensile strength (GPa)	Failure strain (%)	Young's modulus (GPa)
All carbon	1.28	1.39	81.1
Carbon–Kevlar (1 : 1)	0.81	1.51	52.7
All Kevlar	0.64	1.82	33.1

surfaces, as in the case of Fig. 12c, and sometimes the surfaces are angled and show signs of the disrupted internal structure (Fig. 12d). In either event these new failure characteristics could be a direct result of the kind of initial damage shown in Fig. 11f. These pseudo-brittle transverse fractures in the Kevlar fibres are found to occur widely throughout the stressed region of any sample tested in tension–compression cycling modes, as shown by the longitudinal optical micrograph in Fig. 12e. This mode of failure contrasts markedly with the longitudinal splitting characteristic of tensile deformation (Fig. 12f).

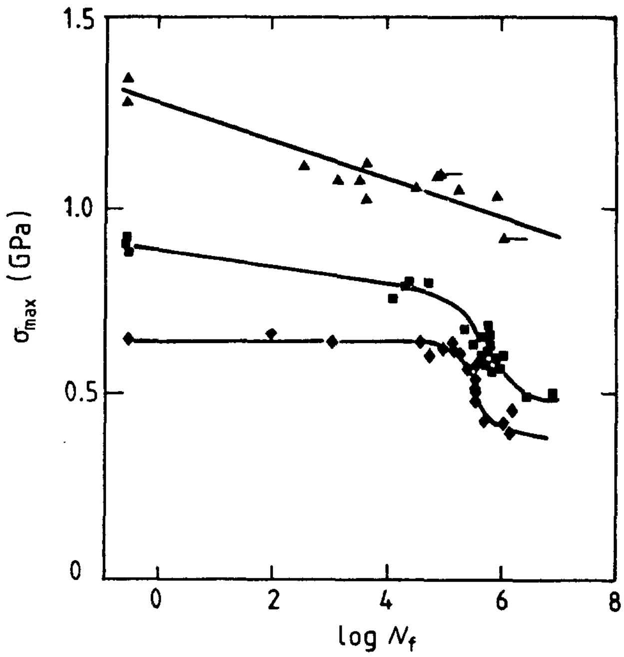

Figure 13 S/log N curves (peak stress) for plain carbon (▲), plain Kevlar (◆), and 50/50 carbon–Kevlar hybrid (■) laminates. Laminate structure is $[(\pm 45, 0_2)_2]_s$ and the fatigue test R ratio is 0.1.

6. Fatigue behaviour of carbon–Kevlar hybrid laminates

The basic mechanical properties of the $[(\pm 45, 0_2)_2]_s$ laminates under discussion here are listed in Table I.

The strength of the all-carbon laminate is 64%, and its modulus 62.3%, of the corresponding values for the unidirectional XAS/914 composite discussed in Section 5. Since 0° plies account for 50% of the cross-section of the laminate, the expected strength and stiffness, on a crude netting analysis basis would be a factor of $\Sigma a_n \cos^4 \theta$ times the unidirectional strength, i.e. 0.625. Agreement with the experimental results for the CFRP laminate is therefore adequate. For the KFRP laminate the agreement is marginally less satisfactory, its strength being 70% and its modulus 58% of the corresponding values for the unidirectional KFRP. The values for the hybrid laminate are all below the means of the results for the single fibre CFRP and KFRP laminates, which are 0.96 GPa, 1.6%, and 57 GPa, i.e. they are, respectively, 84%, 94%, and 92% of the corresponding mixture rule values.

6.1. Repeated tension cycling of $[\pm 45, 0_2)_2]_s$ laminates

Stress–life results for plain carbon, plain Kevlar, and the 50/50 carbon–Kevlar hybrid $[(\pm 45, 0_2)_2]_s$ laminates in repeated tension are shown in Fig. 13. The curve for the plain carbon laminate retains a linear form, as with most unidirectional and 0/90 CFRP composites in repeated tension, and the slope of this curve is 50 MPa per decade, or 3.9% of the static fracture stress per decade. This is close to the value of 4.2% per decade for the unidirectional XAS/914 composites discussed earlier and this, together with the fact that the curve itself shows no deviation from linearity suggests that the presence of the $\pm 45°$ plies has little effect on the fatigue response of the main tensile-load-bearing plies. Unlike the all Kevlar laminate, however, this all-carbon laminate is sensitive to moisture content. The results in Fig. 13 are for the standard moisture content of 1%, but we have observed from a small number of fatigue tests run on dry material that the strength of the dry laminate was only 1.05 GPa, 82% of that of the conditioned material, and that this lower strength persisted in the fatigue response of the dry composite. This difference in behaviour in respect of moisture sensitivity seems likely to be a consequence of the presence of the off-axis plies and the effects of moisture in relaxing residual stresses which would be higher in this material than in others we have studied so far on account of the higher curing temperature. De Charentenay, for example, has suggested [11] that the residual stresses in the $\pm 45°$ plies are a potentially strong source of fatigue cracks in a dry laminate, and it follows that even mild plasticization of the dry resin by water will be likely to have a strong beneficial effect. Presumably the effect is not observed in a plain Kevlar or a hybrid laminate because the residual stresses can be relieved by other mechanisms.

Fig. 13 shows that the results for the all-Kevlar laminate mirror the behaviour of the unidirectional equivalent discussed in Section 5, with the same down-turned curve beyond about 10^5 cycles. The same behaviour is also reflected in the hybrid stress–life curve, as expected. Normalisation of the results in Fig. 13 results in almost complete superposition of all data up to lives of about 10^5 cycles, beyond which only the plain carbon results fall outside the general envelope. This is illustrated in Fig. 14, the data being separated in order to avoid confusion.

We noted earlier that the static strength of the 50/50 hybrid laminate was somewhat below the mean of the strengths of the two single fibre laminates. We now examine the degree of persistence of this effect in the fatigue behaviour of the hybrid laminate. If, from Fig. 13, the fatigue stress for the plain CFRP laminate for a given life, N is taken as $(\sigma_c)_{N2}$, and that for the

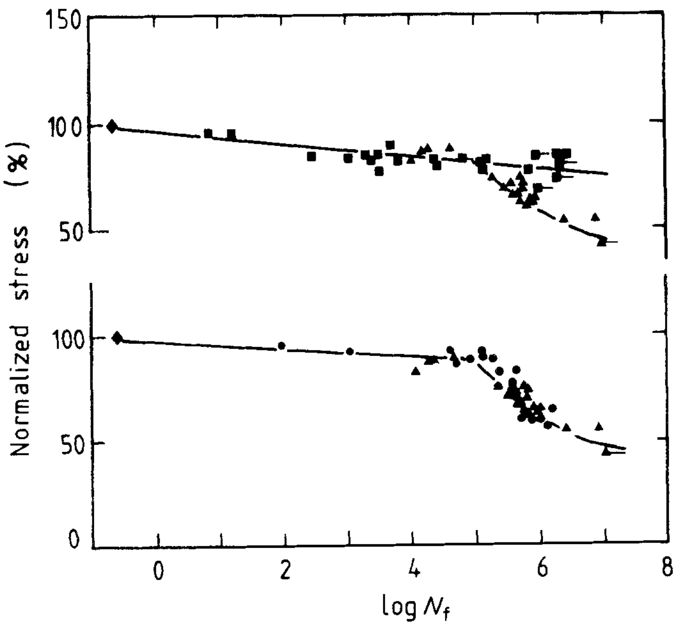

Figure 14 Fatigue results from Fig. 13 plotted on a normalized stress basis (i.e. normalized to the tensile failure stress of the individual laminates). In the upper curve the hybrid (▲) results are compared with those for the equivalent plain CFRP composite (■), and in the lower the hybrid is compared with the plain KFRP equivalent (●) ($R = 0.1$).

plain KFRP laminate is $(\sigma_K)_N$, then the mean value is

$$(\bar{\sigma}_{K,C})_N = \tfrac{1}{2}[(\sigma_K)_N + (\sigma_C)_N]$$

If the corresponding experimental value for the hybrid laminate is $(\sigma_H)_N$, then the extent to which the fatigue resistances of the separate components are translated into the hybrid, using the mixture rule as a basis for comparison, is indicated by the ratio $[(\sigma_H)/(\bar{\sigma}_{K,C})]_N$. The value of this hybrid stress ratio as a function of N is given (as a percentage) in Fig. 15.

From this graph it can be seen that the hybrid retains about 92% of the mean level until a point, between 10^4 and 10^5 cycles, at which the characteristic fall in the KFRP fatigue curve begins to show itself. Beyond this point, the roughly "mixture rule" behaviour of the hybrid is lost. For comparison, Fig. 15 also contains the equivalent information for the unidirectional 50/50 CFRP/KFRP hybrid. It will be recalled that the constant strain model accurately predicts that the strength of this composite will be some 12 or 13% below a "mixture rule" value. It can be seen, however, that under fatigue conditions this situation changes, the dashed curve in Fig. 15 rising towards and beyond the average value (the 100% line) as the fatigue life increases. This suggests that there is a gradual change in the controlling damage mechanism with increasing numbers of cycles, the constant failure strain model becoming increasingly less appropriate. This is, of course, another manifestation of the synergistic effect already demonstrated in Fig. 10.

It seems likely that the difference between the unidirectional and the $[(\pm 45, 0, 0)_2]_s$ behaviour is a result of the presence of the 45° Kevlar plies, since, as already discussed, the 45° carbon plies have no significant effect on the fatigue response of the plain CFRP laminate, apart from reducing its overall load-bearing capacity. However, if the behaviour of the plain KFRP laminates is analysed in somewhat more detail, this argument appears not to be valid. In Fig. 16 we re-plot the curves shown in Figs 4 and 13, respectively, for the unidirectional KFRP and the $[(\pm 45, 0_2)_2]_s$ KFRP laminate together with data for a simple $(\pm 45)_{4s}$ KFRP. The broken line is a mixture-rule prediction for the complex laminate based upon the unidirectional and 45° curves, and it can immediately be seen that the actual laminate test results fall well above the simple

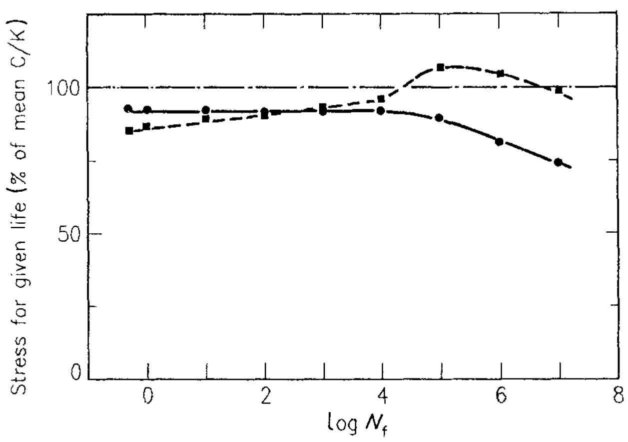

Figure 15 Fatigue behaviour of 50/50 hybrid carbon/Kevlar laminates. The points represent the hybrid fatigue stress for a given life as a percentage of the mean fatigue stresses for the plain CFRP and plain KFRP laminates for the same life. The curve is based on the experimental data of Fig. 6 (for unidirectional samples) (■) and Fig. 13 (for $[(\pm 45, 0_2)_2]_s$ laminates (●)). ($R = 0.1$).

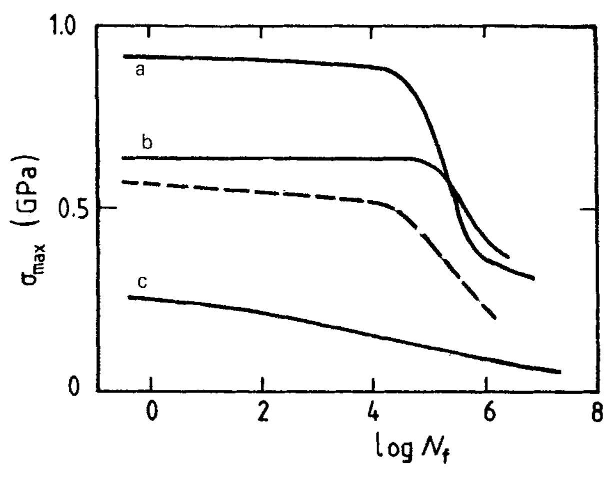

Figure 16 Comparison of the S/log N curves for the plain KFRP laminate (b) (from Fig. 13) with those for the unidirectional plain KFRP (a) composite (from Fig. 4) and results for a $(\pm 45)_{4s}$ laminate (c). The dashed curve represents the mean of the results for the ud and ± 45 materials ($R = 0.1$).

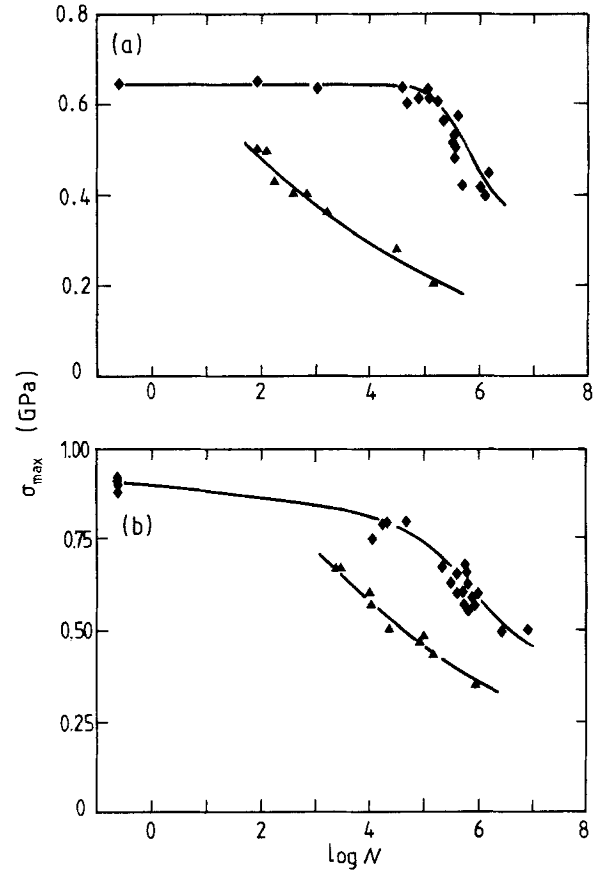

Figure 17 Effect of R-ratio on the S/log N curves (peak stresses) of the (a) plain KFRP and (b) 50/50 hybrid $[(\pm 45, 0_2)_2]_s$ laminates. (◆) $R = 0.1$, (▲) $R = -0.3$.

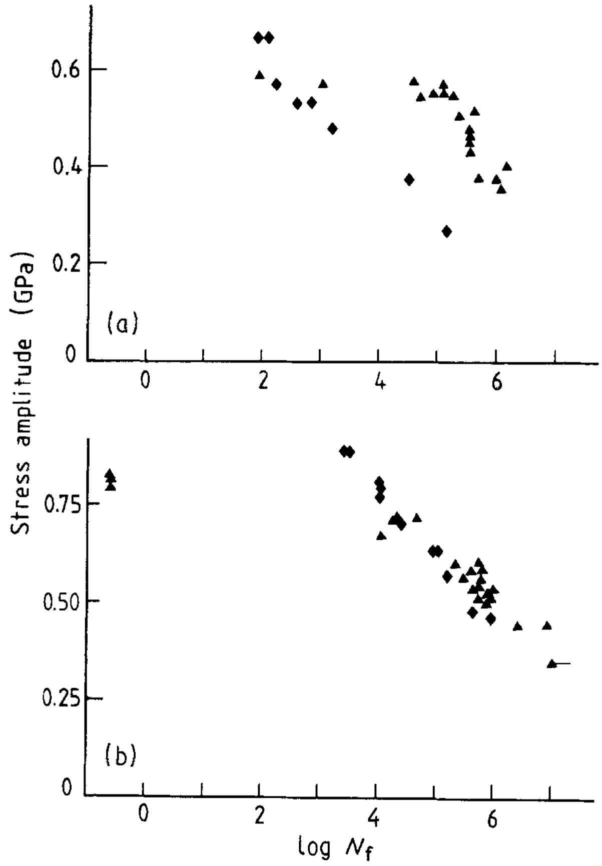

Figure 18 Fatigue results for the (a) plain KFRP and (b) 50/50 hybrid $[(\pm 45, 0_2)_2]_s$ laminates from Fig. 17 replotted in terms of alternating stress range. (◆) $R = -0.3$, (▲) $R = 0.1$.

prediction. From netting analysis, the calculated strength of the $(\pm 45)_{4s}$ laminate (based upon the known unidirectional strength) is 0.23 GPa, which is close to the experimental value of 0.26 GPa. The netting analysis prediction for the $[(\pm 45, 0_2)_2]_s$ laminate is 0.57 GPa, which is close to the mixture rule prediction in Fig. 16 but lower than the experimental strength of 0.64 GPa. This inversion indicates that the known weakness in simple 45° KFRP can be overcome to some extent by appropriate laminate design, and in particular by restricting working strain levels by the incorporation of 0° plies.

6.2. Effect of tension–compression cycling

For these experiments we have concentrated on a tension–compression cycle that was likely to be typical of those met with in aircraft designs, namely, an R ratio of -0.3. The effect of cycling at this R ratio on the stress–life curves for the plain Kevlar and carbon–Kevlar hybrid laminates is shown in Fig. 17. It can be seen that the compressive stress component has had a significant effect on the fatigue response, reducing lives by about two decades for the hybrid, and by even more for the plain KFRP laminate. The S/log N curve for tension–compression cycling gives no indication that the material will show any kind of fatigue limit, unlike the results obtained in repeated tension.

In Fig. 18 the S/log N results given in Fig. 17 have been replotted on a stress-range basis, and as for the unidirectional composites the data for the hybrid laminate at the two R ratios now substantially coincide, indicating that there is no extra susceptibility to compressive fatigue damage in this laminate as a result of the presence of Kevlar plies. It is equally clear, from Fig. 18, that the all Kevlar laminate is at a serious disadvantage in the presence of a compressive load component.

Although we have only limited information on the effect of the R ratio, the results may nevertheless be cross-plotted on a constant life diagram in order to make a more direct comparison with the behaviour of the undirectional carbon–Kevlar hybrids illustrated in the master diagram of Fig. 8. This is done for the plain KFRP laminate in Fig. 19a, where points relating to lives of 10^3, 10^4, 10^5 and 10^6 cycles are shown, together with the 10^5 cycles data from Fig. 9. There is little difference between the two materials for repeated tension cycling, because of the flat shapes of all of the S/log N curves up to lives of 10^5 cycles, and the points at the top end of the $R = 0.1$ line are closely bunched, well within the scatter of the individual curves. The effect of the compression component of stress, however, is to increase the separation of the points for the different lives, as could be judged from the S/log N curves themselves. Direct comparison of the two sets of points for 10^5 cycles shows the much more marked effect of the compression component on the laminate resulting from the presence of the 45° plies. As would be expected, the behaviour of the 50–50 hybrid laminate contrasts strongly with this pattern of behaviour, as shown in Fig. 19b, the data for the laminate now being well separated from those for the much more

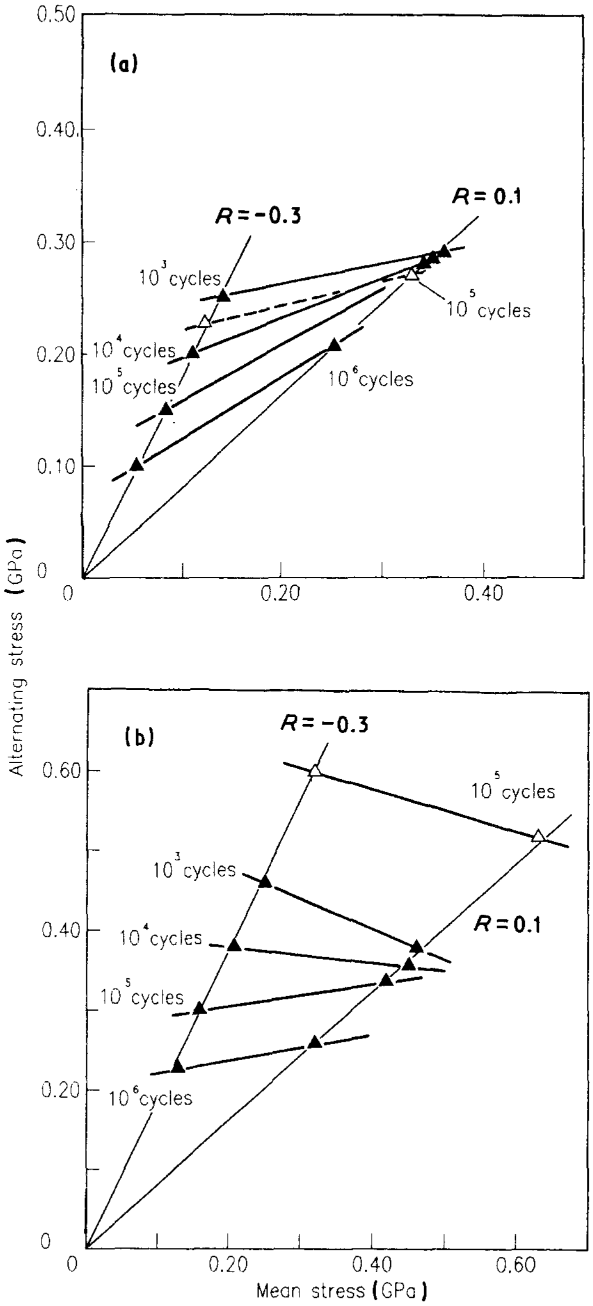

Figure 19 Constant life diagram segments for (a) plain KFRP and (b) 50/50 C/K hybrid unidirectional (△) and $[(\pm 45, 0_2)_2]_s$ (▲) laminates.

resistant unidirectional hybrid and the slopes of the lines for 10^5 cycles being of opposite sign, as with the plain KFRP composites. These differences serve to emphasize further the points of difference that we observe in the repeated tension response of the three families of $[(\pm 45, 0_2)_2]_s$ laminates.

7. Conclusions

The fatigue stress (for a given life) of unidirectional CFRP–KFRP hybrid composites varies linearly with composition: since the tensile strength of these composites does not vary linearly with Kevlar content, this implies that the fatigue ratio, which is perhaps the more useful comparative design parameter, shows what is commonly referred to as a positive synergistic effect.

Whether this is a valid statement, or simply an indication that there is no appropriate model for the fatigue behaviour of hybrids, it is clear that Aramid fibres, which are normally considered to exhibit deficiencies in their response to fatigue and to compressive stresses, exert no undue weakening effect on the fatigue response of CFRP–KFRP hybrids.

Fractographic studies provide evidence for the validity of the model of Talreja in respect of microstructural damage mechanisms during fatigue cycling. In plain KFRP fatigue damage results in core-skin separation and pull-out of the Aramid fibres. In hybrids, however, this mechanism is suppressed, and the Kevlar fibre plies exhibit the same kind of planar failure as the CFRP plies.

Similar conclusions can be drawn in respect of the behaviour of $[(\pm 45, 0_2)_2]_s$ hybrid laminates. Although in plain KFRP $(\pm 45)_{4s}$ composites, the weakness of the Kevlar fibres in shear is clearly manifest, the presence of CFRP plies is protective, and the hybrid laminates show no evidence of any weakening as a result of the presence of the organic fibre, whether in repeated tension cycling or in tension–compression cycling.

Acknowledgements

The authors are grateful to the Procurement Executive (MoD) for sponsorship of this work and to Dr P. T. Curtis and Dr G. Dorey of the Royal Aircraft Establishment, Farnborough, for their advice and interest during the execution of the program. We are also pleased to acknowledge the work of the Electron Optics Centre at the University of Bath for the production of electron micrographs.

References

1. L. N. PHILLIPS, "Proceedings of the Reinforced Plastics Congress, Brighton" (British Plastics Federation, London, 1979) pp. 207–211.
2. K. E. HOFER, M. STANDER and L. C. BENNETT, *Polym. Engng Sci.* **18**, (1978) 120.
3. K. E. HOFER, N. RAO and M. STANDEN, "Proceedings Second International Conference on Carbon Fibres", (Plastics Institute, London, 1974) pp. 201–212.
4. N. J. PARRATT and K. D. POTTER, "Advances in Composite Materials" Vol. 1, Edited by A. R. Bunsell, C. Bathias, A. Martrenchar, D. Menkes and G, Verchery (Pergamon, Oxford, 1980) pp. 313–326.
5. C. J. JONES, R. F. DICKSON, T. ADAM, H. REITER and B. HARRIS, *Proc. R. Soc.* **A396**, (1984) pp. 315–338.
6. R. TALREJA, *Proc. R. Soc.* **A378**, (1981) pp. 461–475.
7. T.-W. CHOU and A. KELLY, *Ann. Rev. Mater. Sci.* **10**, (1980) pp. 229–259.
8. M. R. PIGGOTT and B. HARRIS, *J. Mater. Sci.* **15** (1980) pp. 2523–2538.
9. G. KRETSIS, *Composites* **18**, (1987) pp. 13–23.
10. M. J. OWEN and S. MORRIS, in "Carbon Fibres: Their Composites and Applications" (Plastics Inst., London, 1971) pp. 292–302.
11. F. X. de CHARENTENAY, P. SAUVE, G. BEHAR, K. KAMIMURA and J. M. CHOPIN, "Comptes Rendus des Troisièmes Journées Nationales sur les Composites" (Editions Pluralis, Paris, 1982) pp. 151–158.

Received 11 November 1987
and accepted 3 March 1988